

Case Study of Tsunami Evaluation Triggered by Submarine Landslide

Yoshikane MURAKAMI*, Takemi SHIKATA**, Koji TONOMO**

*Centers for Civil Engineering and Architectures, Kansai Electric Power Co., Inc.

**Port and Coastal Engineering Group, Newjec Inc.

(Received: Feb.2, 2018 Accepted: May.10, 2018)

Abstract

It is necessary to establish a consistent evaluation scheme for estimating the height of tsunamis triggered by submarine landslides, since a standard framework for evaluation has not been established even though several models for calculation have been proposed and applied in practice. In this study, we propose a method of evaluating the height of a tsunami triggered by a submarine landslide using three schemes – the KLS model, Watts model and modified-KLS model for calculation, by setting the detailed profile of the submarine landslide based on the marine geological map and reanalysis of the marine acoustic wave exploration records. As a result of the comparison of the tsunami height evaluation produced by each model, it was suggested that, comparing the experimental result and those of other methods, a safe-side evaluation result might be obtained by the KLS model, applying the maximum sliding velocity calculated by the Watts model as a parameter.

Keywords: submarine landslide, landslide-triggered tsunami, tsunami height evaluation, new regulatory requirements for nuclear power plants, standard tsunami

1. INTRODUCTION

In cases of tsunami triggered by submarine landslide, it is reported that although the frequency of occurrence is exceptionally low compared with the more common seismic tsunami triggered by marine fault activity, these may nonetheless on rare occasions inflict extensive damage, such as in the 1771 Meiwa-Yaeyama earthquake tsunami. According to Hiraishi et al. (2001), the tsunami trace height in the southern part of Ishigaki Island reached about 30 m, about 40% of the area of the island was inundated and more than 10,000 people were drowned by the tsunami. It is difficult to explain the tsunami height only by fault displacement based on the seismic scale, and reproduction calculations applying the circular slip method have shown that the tsunami might have been triggered by a submarine landslide. According to Matsuyama et al. (2001), the 1998 Papua New Guinea tsunami could also be a tsunami triggered by a submarine landslide based on reproduction calculations applying the calculation method proposed by Grilli et al. (1999).

Since traces of numerous submarine landslides have been discovered in the sea around Japan, the possibility of future occurrences cannot be excluded. Therefore, it is expedient to consider relevant submarine landslides as a factor in evaluating tsunami impacts on coastal structures, based on the topographical characteristics of the evaluated site. For example, taking into account the lessons learnt from the nuclear accident triggered by the Great East Japan Earthquake and the following huge tsunami, the Nuclear Regulation Authority was established, and the new regulatory requirements, which are the most stringent in the world, went into effect (Agency for Natural Resources and Energy, 2014). In the review of conformity to these requirements, it is a requirement to establish a site-specific “standard tsunami” based on numerical analysis, allowing for uncertainties such as source location, scale and occurrence timing etc., considering general seismic faults, non-seismic factors and combinations thereof selected as the source of the tsunami.

As a standard framework for evaluation has not been established (although several models for calculation have been proposed and applied in practice), it is important to establish a consistent evaluation scheme for submarine landslides. In this study, we propose a consistent method of tsunami height evaluation applicable to future submarine landslides.

2. PROCEDURE FOR EVALUATING A SUBMARINE LANDSLIDE TSUNAMI

To evaluate the possibility of a tsunami triggered by a submarine landslide in the waters surrounding Wakasa Bay, we carried out the following procedure based on the available marine geological map and reanalysis of the marine acoustic exploration records. Wakasa Bay, about 100 km north of Osaka, is a ria coastal area of about 2,700 km², which formed as the pre-existing valley topography was submerged by the rising sea levels of the Sea of Japan.

On the coast of Wakasa Bay, 14 nuclear power plants are located. As a tsunami may have the potential to affect these power plants, the scale of submarine landslides and the heights of possible tsunamis were estimated. The distribution of submarine landslides was confirmed based on detailed reviews of sedimentological and marine geological maps, such as those by Tokuyama et al. (2001), Yamamoto et al. (1989) and Katayama et al. (1993).

(1) Specify the features of the submarine landslide topography

The features of the possible submarine landslide topography were specified by interpreting the submarine topography prepared using a digital bathymetric chart. In interpretation, the typical features of collapsed and sedimentary parts of the possible submarine landslide topography and the overall concepts of these pairs were taken into consideration. These criteria are summarized in Table 1. Then, the marine acoustic exploration records were interpreted, and the strata were classified based on the classification of Ikehara et al. (1990) in order to ascertain the presence of submarine landslides.

Table 1. Key criteria for judgment of landslide extraction in submarine topography interpretation

Viewpoint	Typical features
Overall concept	<ul style="list-style-type: none"> ✓ Slump scarp and sliding soil mass deposited on its base are paired. ✓ It tends to spread on a large scale and thinly compared to onshore landslides. Only slump scarps are specified in the case where it is difficult to specify the extent of sliding soil mass.
Collapsed part (slump scarp)	<ul style="list-style-type: none"> ✓ 'Horseshoe' shape or 'semi-circle' shape on the steep slope, the lower side is wider. ✓ Smooth planar shape, constant inclination. ✓ Deposited paired sliding soil mass downward.
Sedimentary part (sliding soil mass)	<ul style="list-style-type: none"> ✓ 'Fan' shaped or 'tongue' shaped thin mound at the base of the slump scarp. ✓ In some cases, it may be an elongated tongue or a plateau. ✓ In typical cases, there are irregular undulations, low cliffs and depressions on the surface of the sliding soil mass indicating a convex vertical profile.

(2) Scale estimation of submarine landslide topography

The location area of the specified submarine landslide topography was divided into groups in consideration of the position and orientation, with a view to thoroughly extracting candidate sources of tsunamis that could seriously affect Wakasa Bay. Then, the scale of each tsunami was estimated based on the estimated vertical cross-sectional area of the collapsed part. In order to calculate topographical changes due to a submarine landslide in detail, the collapsed and sedimentary parts of the sea bottom topography judged to be the largest submarine landslide in each divided area were interpreted based on a reanalysis of the acoustic exploration record in the relevant sea area.

(3) Tsunami height estimation

The initial sea level distribution of the tsunami to be induced by the submarine landslide was estimated by using three different models (i.e., KLS model, Watts model, and modified-KLS model) as described later. The tsunami propagation was calculated according to nonlinear long wave theory and the height of the tsunami was estimated.

3. SETTING OF SUBMARINE LANDSLIDE PROPERTIES TO BE EVALUATED

3.1 Detection and extraction of the submarine landslide traces

According to Tokuyama et al. (2001), a group of submarine landslide traces is shown near the Oki Trough of the Japan Sea. Also, several possible slump scarps are shown extensively around the Oki Trough in the marine geological map provided by the National Institute of Advanced Industrial Science and Technology (e.g. Yamamoto et al., 1989). According to the sedimentological map (e.g. Katayama et al., 1993), the facies suspected of submarine landslides are shown around Oki Trough in the same way. Slump scarps and facies suspected of submarine landslides are not shown in other areas.

Based on the results of these literature surveys, we ascertained the presence of submarine landslide topography by reanalyzing the results of high-resolution marine acoustic exploration records for all sea areas around Oki Trough, where there might be a submarine landslide topography. As a result, a total of 38 submarine landslide traces were extracted on the continental slope near the southeastern and southwestern parts of Oki Trough, about 500 m to 1,000 m in depth.

In addition, a little offshore of the entrance of Wakasa Bay, there is a distinctive geomorphic feature called Echizen Bank Chain, which is a scattering of rock reefs and large shallows at depths of 50 m to 100 m. According to the marine geological map, slump scarps suggesting a submarine landslide are not shown, but a reverse fault is shown along the southeast edge of Echizen Bank Chain. We also reviewed the marine acoustic exploration records, and did not recognize a turbulent sedimentary structure suggesting a submarine landslide.

3.2 Selection of submarine landslide topographies to be evaluated

The 38 submarine landslide traces extracted as study targets were broadly classified into three areas (Areas A to C) depending on their locations and orientations as shown in Fig. 1, since the submarine landslide traces in Oki Trough are distributed over a vast area and a tsunami triggered by the largest scale landslide would not necessarily impact on Wakasa Bay the most severely. Area A is a group located virtually true north of Wakasa Bay, consisting of 9 slump scarps. Area B is a group located northwest of Wakasa Bay and consists of 8 slump scarps whose central axes are virtually oriented in the direction of Wakasa Bay. Area C is a group located further northwest of Area B, consisting of 21 slump scarps, which are situated entirely behind Tango Peninsula in relation to Takahama Nuclear Power Plant.

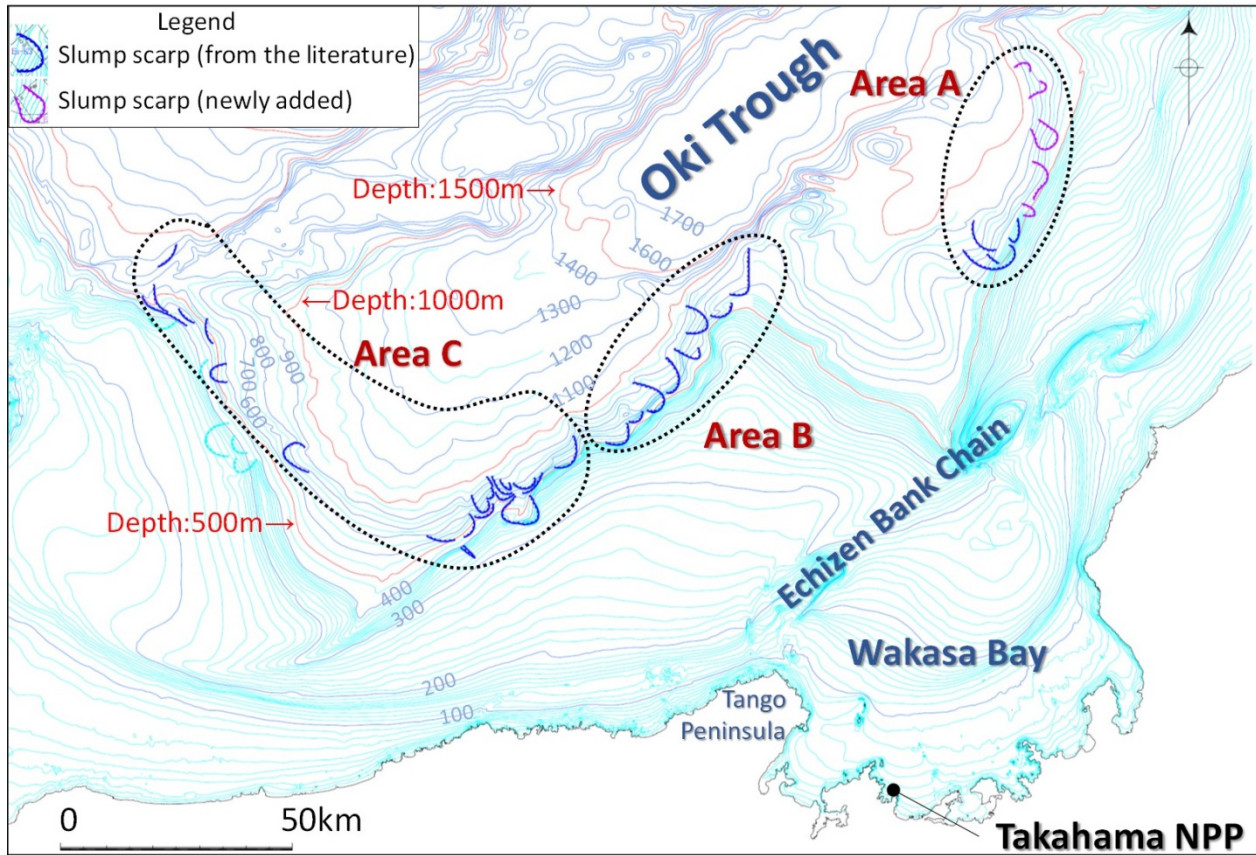


Fig. 1. Location map of 38 extracted submarine landslide traces

With regard to the submarine landslide of Area A, located north of Wakasa Bay, Yamamoto (1991) mentioned that "This submarine landslide trace (=Area A) was formed by two slope failures. The collapse is thought to have occurred at the time of declining sea levels during the last ice age, and the trigger for the collapse may have been an increase in the inclination angle due to a developing anticline structure, and an increase in the supply of sediment to the slope area." In other words, it is impossible to accurately estimate a future submarine landslide, since the geological environment around Oki Trough is totally different from that in the past. Therefore, we decided to evaluate, for each area, the tsunami triggered by the largest landslide from the extracted traces of earlier submarine landslides. Using this approach, we expected to comprehensively estimate, on the safe side, for tsunami height evaluation, even allowing for uncertainties – the possibility that a future submarine landslide will occur on a different scale and in a different place.

Since vertical water level fluctuations have a high impact on tsunami height estimation, we considered the largest submarine landslide to be the submarine landslide topography with the largest vertical cross section of the collapsed part, estimated from the high-resolution marine acoustic exploration records for the respective areas. Regarding the validity of the method of scale evaluation based on the cross-sectional area applied in this study, it is confirmed that the same landslide topography is selected as the largest scale, even in the case where the estimated volume of the collapsed part is calculated by multiplying the projected area of the slump scarp by the maximum thickness, interpreted from the high-resolution marine acoustic exploration records.

Based on the above, the largest submarine landslide topography of the respective areas was selected as shown in Fig. 2 to be evaluated.

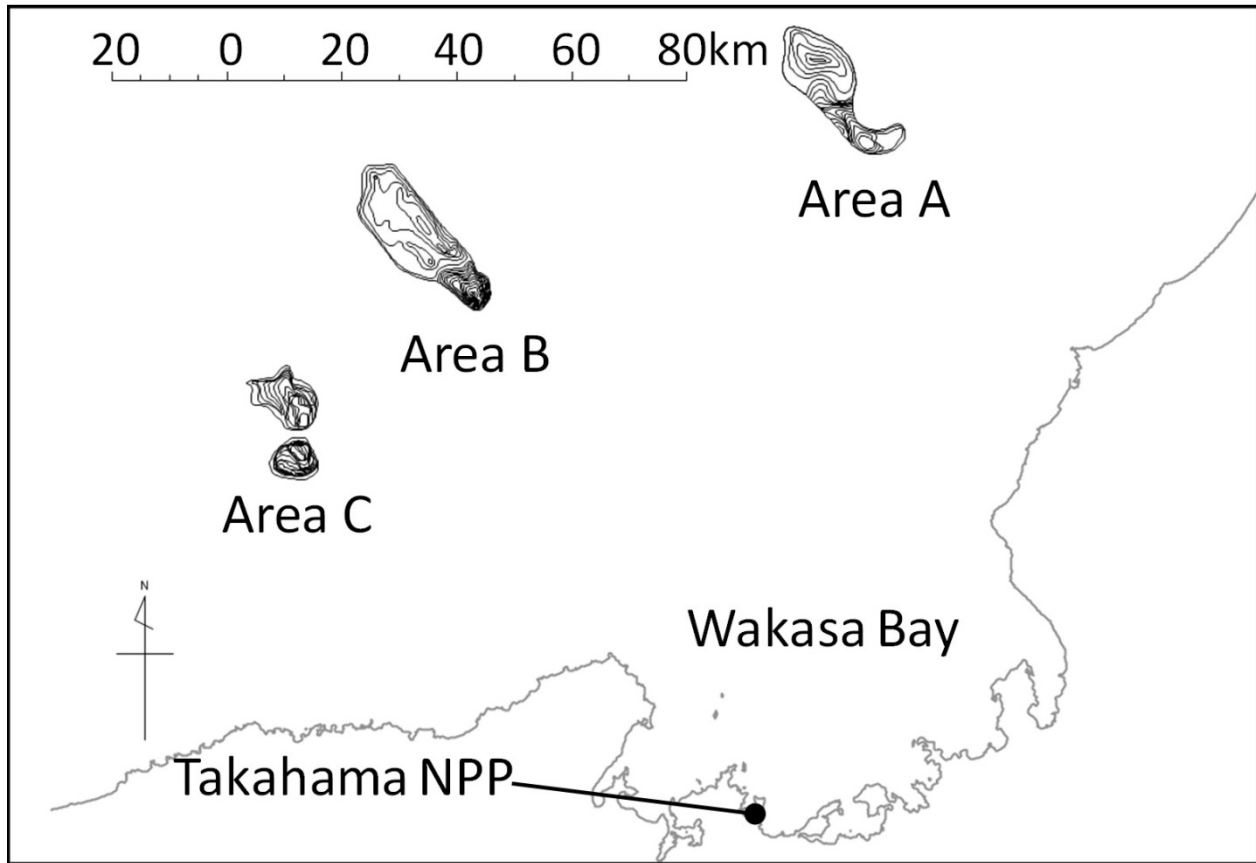


Fig. 2. Selected largest submarine landslide topography of respective areas

3.3 Estimation of topographical change caused by submarine landslide

The topographical change of the sea bottom due to a landslide is estimated according to the following procedure (Fig. 3) in accordance with Yamamoto (1991) based on high-resolution marine acoustic exploration records, since it needs to be estimated accurately as it is considered to directly affect tsunami height.

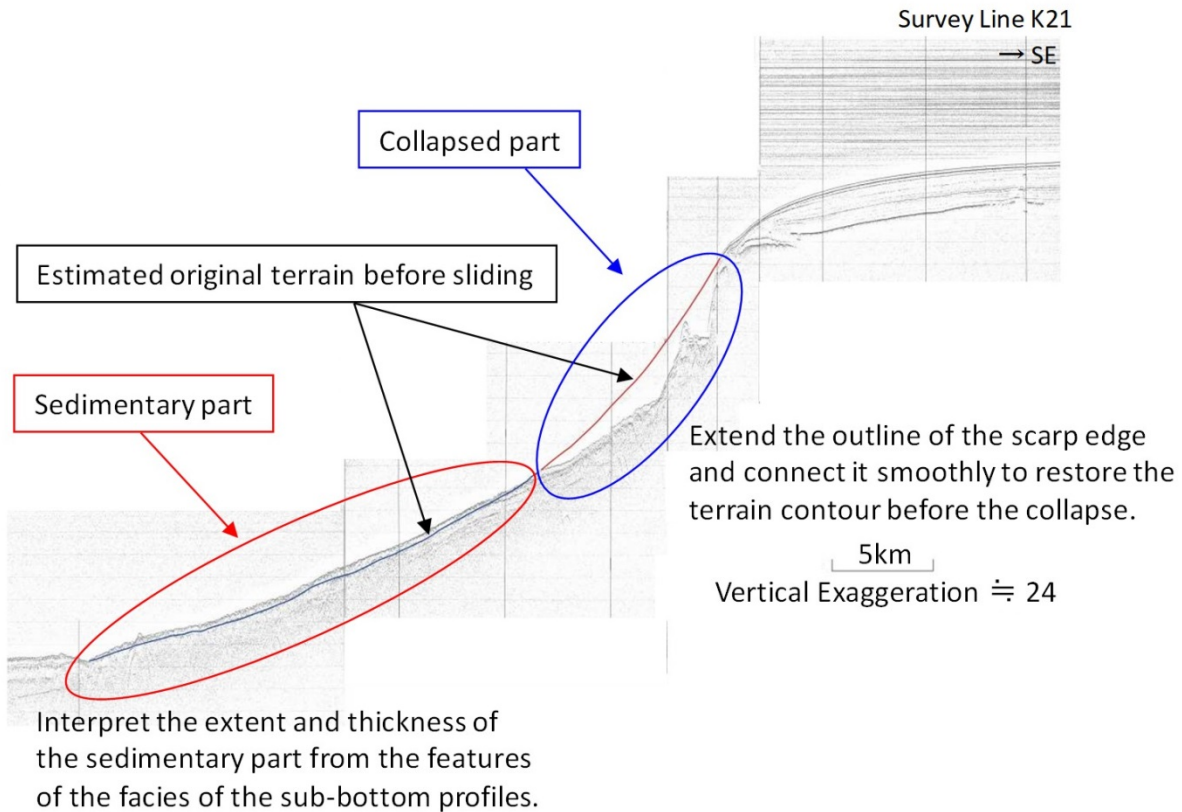


Fig. 3. Typical example of interpretation of the sea bottom topographical change due to submarine landslide

- i) Reanalyze the high-resolution marine acoustic exploration records and interpret the width, length, altitude etc. of the collapsed and sedimentary parts from the features of the facies of multiple sub-bottom profiles passing through the submarine landslide topography.
- ii) To restore the terrain contour before the collapse, extend the outline of the scarp edge and connect it smoothly, cross-check between each of the survey lines, and confirm the three-dimensional consistency of the restored terrain contour.
- iii) Considering the balance between the volume of collapsed and sedimentary parts, estimate the distribution of the volume of topographical change of the sea bottom.

Applying the above procedure to the submarine landslide in Area A interpreted by Yamamoto (1991) produced substantial consistency with Yamamoto's results in the restored topography before the collapse, the distribution of the sea bottom topographical change and the collapse volume, and confirmed that the procedure is reasonable. The above procedure was then also applied for Areas B and C to estimate the change in the sea bottom topography. Figures 4-1 to 4-3 show the estimated distribution of the sea bottom change due to the submarine landslide and marine acoustic wave exploration records along typical survey lines.

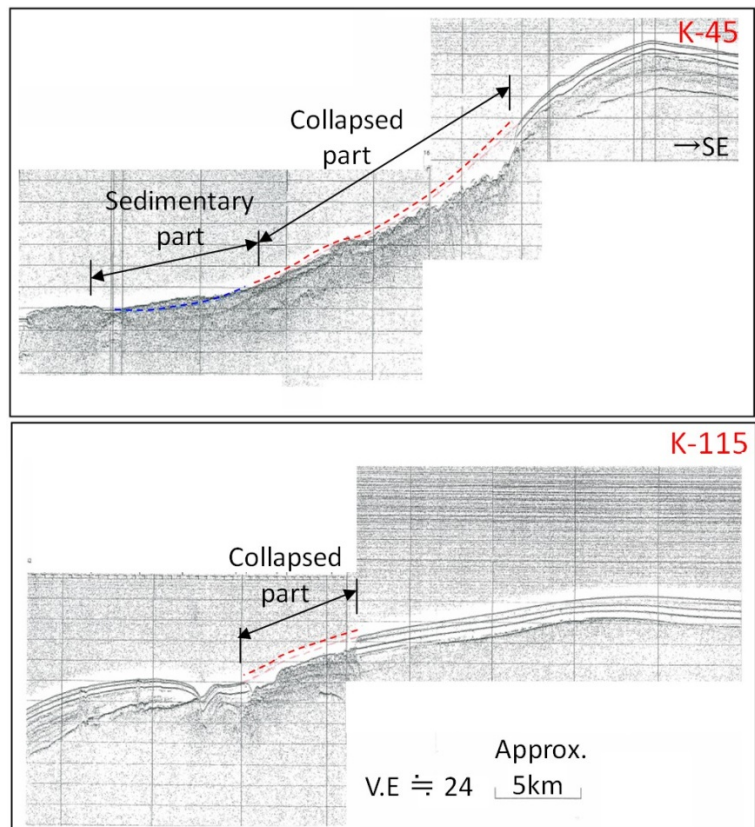
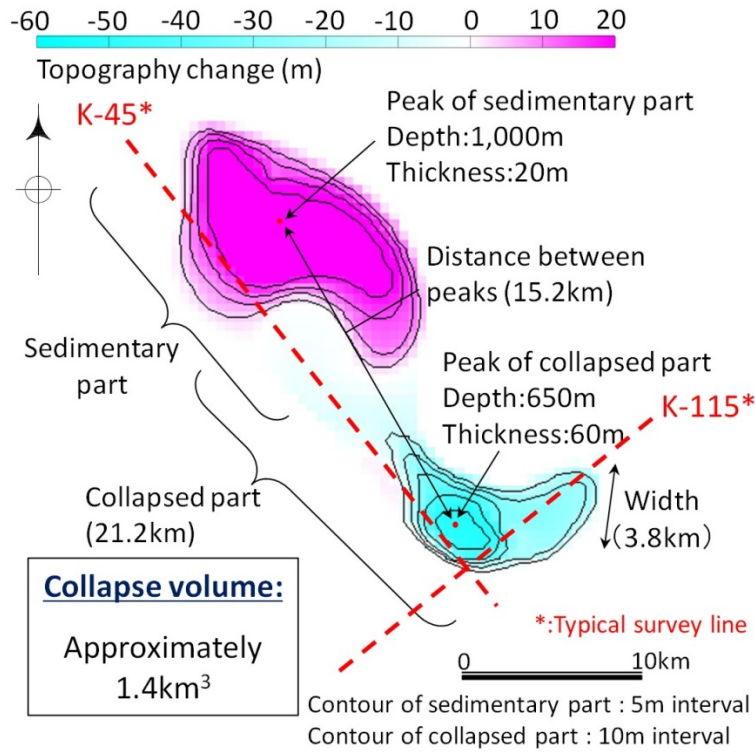


Fig. 4-1. Estimated distribution of the sea bottom change due to submarine landslide and marine acoustic wave exploration record along the typical survey lines (Area A)

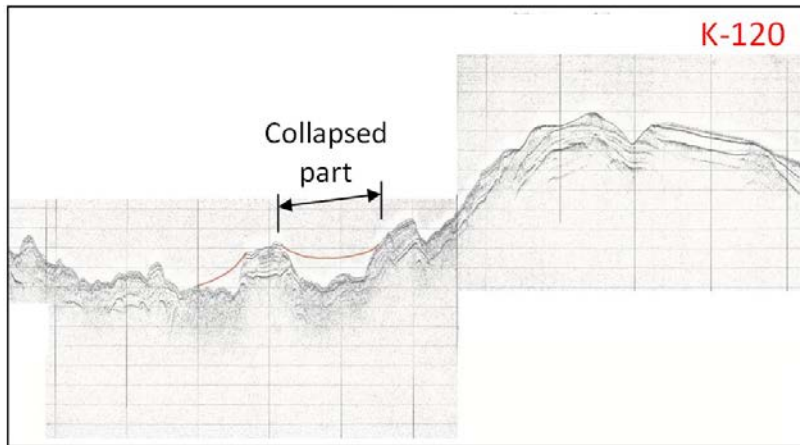
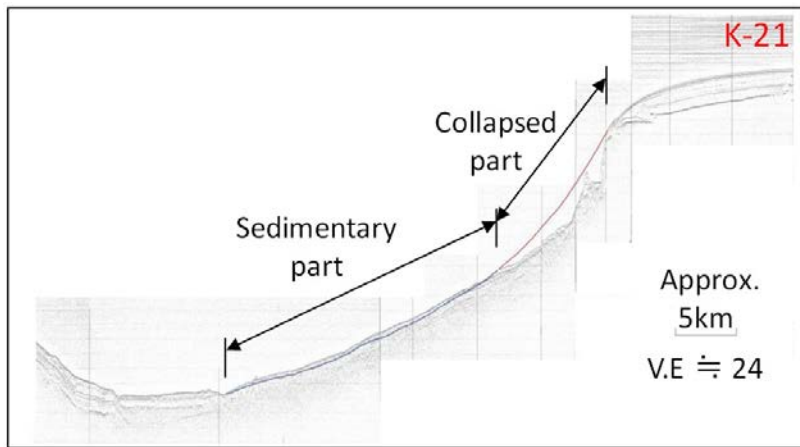
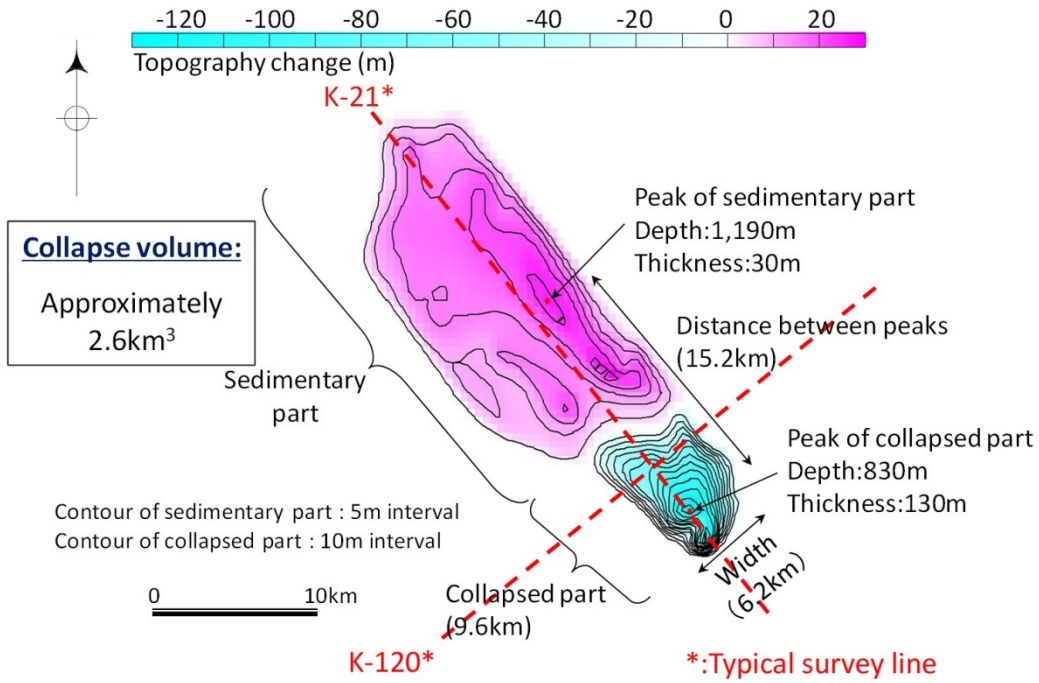


Fig. 4-2. Estimated distribution of the sea bottom change due to submarine landslide and marine acoustic wave exploration record along the typical survey lines (Area B)

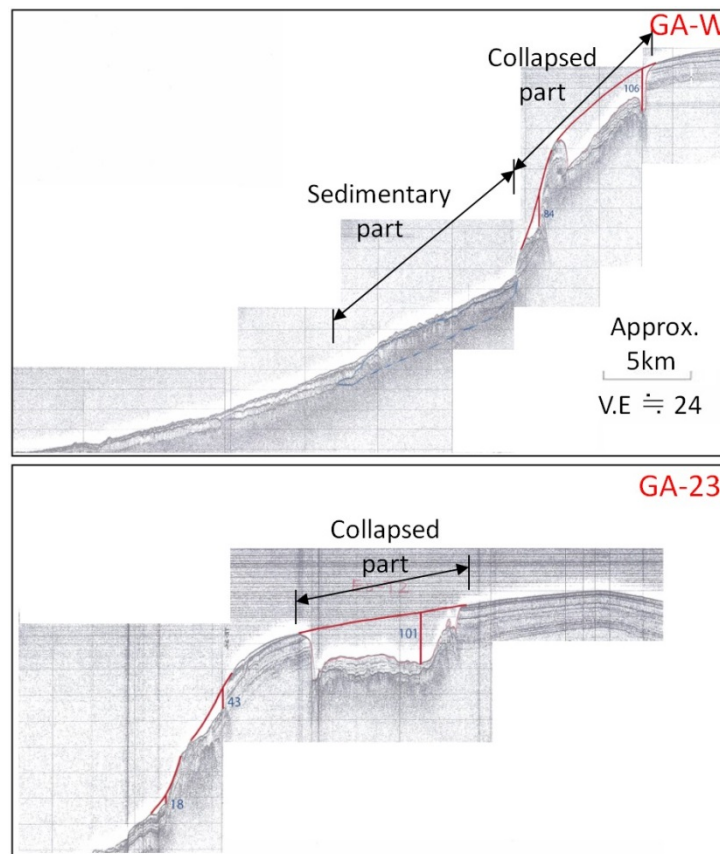
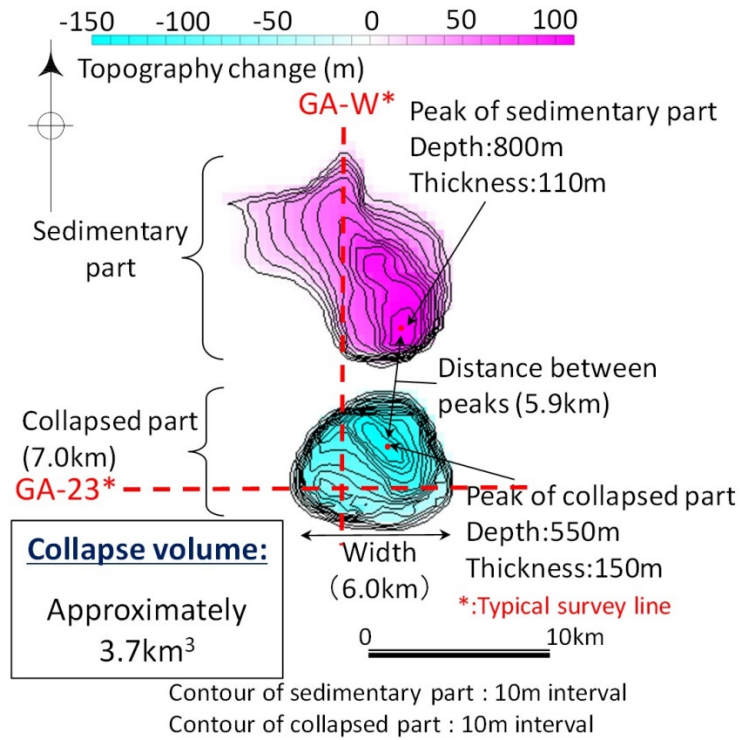


Fig. 4-3. Estimated distribution of the sea bottom change due to submarine landslide and marine acoustic wave exploration record along the typical survey lines (Area C)

4. ESTIMATION OF TSUNAMI HEIGHT TRIGGERED BY SUBMARINE LANDSLIDE

4.1 Approach for tsunami height estimation

To estimate the height of a tsunami triggered by a submarine landslide, tsunami propagation simulation was carried out with the condition that the initial water level distribution was calculated based on the original sea bottom topography and the collapsed topography after the landslide.

The initial water level distribution was calculated by more than one forecasting approach in consideration of uncertainty. The kinematic landslide model (KLS model) proposed by Satake and Kato (2002), Watts model proposed by Watts et al. (2005) and Grilli et al. (2005) and the modified-KLS model proposed by the authors (Tonomo et al., 2015) were applied to set the initial condition for the tsunami propagation simulation.

(1) KLS model

Based on the calculation model proposed by Satake and Kato (2002) as shown in Fig. 5, the topographical change before and after the landslide is considered as propagating at sliding velocity 'U' from the single rupture starting point (peak of the collapsed part), and the topographical change of each calculation point is considered as continuing for duration time 'Tz'. Next, the tsunami propagation simulation is carried out with the condition that this topographical change amount (change amount per unit calculation time) is considered as being directly reflected in the sea bottom topography and sea level.

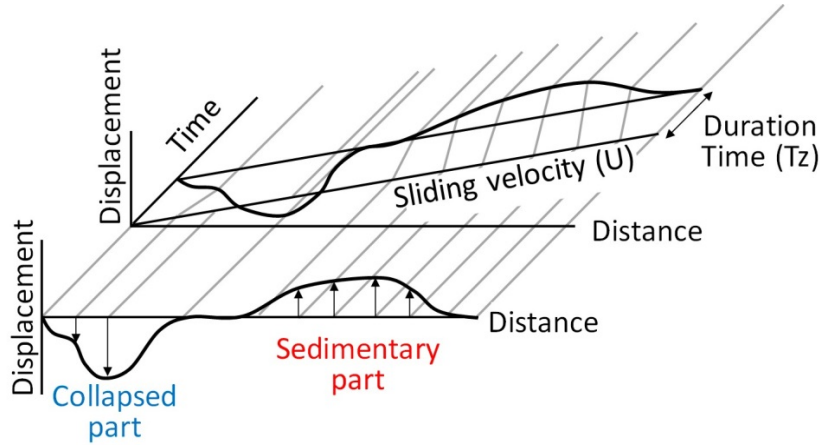


Fig. 5. Conceptual overview of the KLS model proposed by Satake and Kato (2002)

Currently, there is no established knowledge to set the required parameters 'U' and 'Tz' in general. Therefore, in accordance with our previous study (Tonomo et al., 2015), we applied the maximum landslide velocity obtained by the estimation formula, shown as U_{max} in Eq. (1), proposed by Watts et al. (2005) as sliding velocity 'U' in this study. As for the duration time 'Tz', we applied the calculated value obtained from Eqs. (2) and (3) based on the landslide velocity U_{max} so that the duration time would be the fastest in the range in which the topographical change is considered reasonable. Also, the completion time of the landslide, 'T_{end}', can be calculated as shown in Eq. (4).

$$U = \sqrt{gd} \sqrt{\frac{b \sin \theta}{d} \frac{\pi(\gamma-1)}{2C_d} \left(1 - \frac{\tan \psi}{\tan \theta}\right)} \quad (1)$$

$$T_z = D_z / U_z \quad (2)$$

$$D_z = T / \cos \theta, \quad U_z = U \sin \theta \quad (3)$$

$$T_{end} = T_z + (h-d) / U_z \quad (4)$$

Where, b : length of sliding mass, d : initial depth of sliding mass, T : thickness of sliding mass, θ : slope angle, Ψ : friction angle, γ : specific gravity of sliding mass, C_d : drag coefficient, D_z : maximum collapse depth, U_z : sliding velocity (vertical component), h : water depth.

(2) Watts model

Whereas the above-mentioned KLS model calculates the time series change of the sea bottom topography and sea surface fluctuation simultaneously for every time unit, the Watts model is a relatively simple scheme, in that it calculates tsunami propagation by using as the initial condition the initial spatial distribution of the water level due to the landslide.

To adopt the Watts model, it is necessary to properly define the initial water level distribution. In this study, we considered applying the proposed formula of Watts et al. (2005) and Grilli et al. (2005) based on Tonomo et al. (2015). The proposed equations are shown in Eqs. (5) and (6).

$$\eta(x, y) = -\frac{\eta_{0,3D}}{\eta_{\min}} \operatorname{sech}^2 \left(\kappa \frac{y - y_0}{w + \lambda_0} \right) \left(\exp \left\{ -\left(\frac{x - x_0}{\lambda_0} \right)^2 \right\} - \kappa' \exp \left\{ -\left(\frac{x - \Delta x - x_0}{\lambda_0} \right)^2 \right\} \right) \quad (5)$$

$$\eta_{0,3D} = \eta_{0,2D} \left(\frac{w}{w + \lambda_0} \right) \quad (6)$$

Where, $\eta_{0,3D}$: maximum water level decrease (three-dimensional), w : width of Submarine Mass Failure (SMF), η_{\min} : minimum of the function on the right-hand side of Eq.(5) excluding the amplitude, κ ; κ' : shape parameters ($\kappa=3$). In addition, the parameters w , η_0 , D , λ_0 : characteristic tsunami wave length and Δx ($=\lambda_0/2$), which are required for the proposed equation are obtained from the result of interpretation of the collapsed topography, or calculated from the prediction equation of the tsunami amplitude as shown below.

$$t_0 = \sqrt{\frac{R}{g}} \sqrt{\frac{\gamma + C_m}{\gamma - 1}} \quad (7)$$

$$\lambda_0 = t_0 \sqrt{gd} \quad (8)$$

$$\eta_{0,2D} = S_0 \left(\frac{0.131}{\sin \theta} \right) \left(\frac{T}{b} \right) \left(\frac{b \sin \theta}{d} \right)^{1.25} \left(\frac{b}{R} \right)^{0.63} (\Delta \Phi)^{0.39} \{1.47 - 0.35(\gamma - 1)\} (\gamma - 1) \quad (9)$$

Where, b : length of SMF, d : initial depth of SMF, T : thickness of SMF, θ : slope angle, γ : specific gravity of SMF, X_g : coordinates of the position where the initial water depth is d , C_m : additional mass coefficient ($=1$), S : moving distance, S_0 : characteristic distance ($=S/2$), R : curvature radius ($=b^2/8T$), $\Delta \Phi$: rotation angle ($=2S_0/R$), t_0 : characteristic time, $\eta_{0,2D}$: maximum water level decrease amount at $X = X_g$. In addition, the symbols of the parameters applied for the Watts model used here are as shown in Fig. 6.

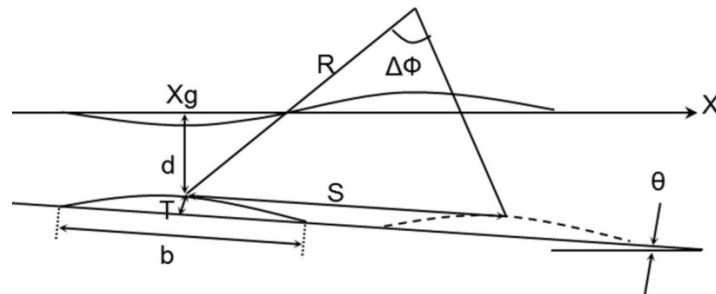


Fig. 6. Symbol of the parameters applied for the Watts model

(3) Modified-KLS model

Regarding the validity of the tsunami height evaluation, we conducted a reproduction calculation of the submarine landslide model experiment implemented by Hashimoto and Dan (2008) using the KLS model and the Watts model (Tonomo et al., 2015). According to this, the KLS model has an excessive result of about 1.5 to 3 times the tsunami height compared with the experimental results in all verification cases. On the other hand, the reproducibility of the Watts model was good, especially in the case where the slope angle was relatively small (6° or less). In this study, based on the slope angle of Area B being as little as 1.7° , it is considered that the Watts model is more appropriate than the KLS model from the viewpoint of tsunami height evaluation.

The reason for the calculation result using the KLS model being excessive compared with the experimental result is presumed to be that the sediment volume between the collapsed and sedimentary parts is imbalanced in the landslide duration time. In the case where the KLS model was applied to the submarine landslide, collapse proceeds until the front edge of the sliding mass reaches the sedimentary part, since a single rupture starting point is set in the collapsed part. This is due to the fact that the KLS model is fundamentally a computational model devised for tsunami height estimation triggered by onshore landslide (collapse of volcanic edifice).

In order to solve this matter, we proposed using the modified-KLS model reported by the authors (Tonomo et al., 2015). This model is designed such that collapse and sedimentation proceed simultaneously to keep the balance of the sedimentation volume between the collapsed and sedimentary parts in the landslide duration time. To achieve this goal, the rupture starting point was set at two locations in both the collapsed part and the sedimentary part. In addition, the landslide velocity applied to the modified-KLS model was set to 1/2 of the KLS model from the consideration that the landslide completion time should be the same for both models. The concept of the difference between the KLS model and the modified-KLS model is shown in Fig. 7. As a result, the modified-KLS model showed that the experimental results can be reproduced well from the viewpoint of tsunami height evaluation.

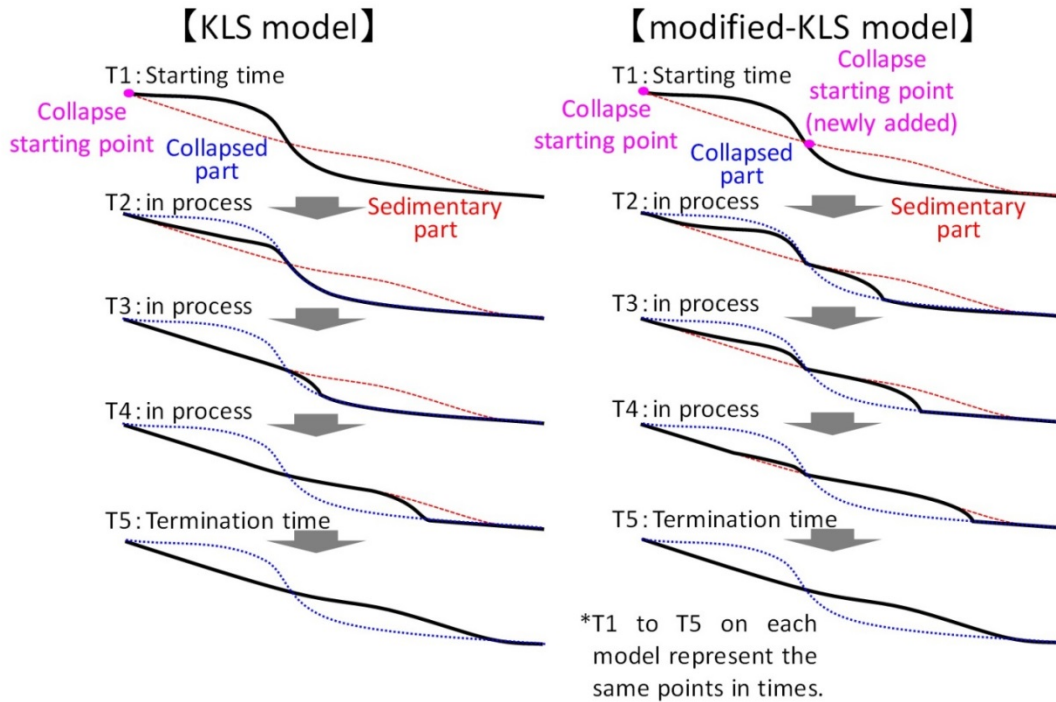


Fig. 7. Illustration of the concept of the difference between the KLS model and the modified-KLS model

(4) Calculation conditions and detailed parameters

Tsunami propagation simulation was carried out on the above-introduced calculation schemes, applying the parameters of each of the submarine landslides in Areas A to C established in Chapter 3. The parameters and initial spatial water level distribution in the Watts model are shown in Table 2 and Fig. 8. Table 3 shows the calculation conditions applied to the KLS model in Areas A to C, and Figures 4-1 to 4-3 show the distribution of the topographical change amount input to the KLS model. Figure 9 shows the time series variation of topographical change, and tsunami propagation calculated by KLS model in Area B from immediately after the topographical change triggered by the sliding until about 16 minutes after the topographical change is completed.

Table 2. Parameters applied to the Watts model

Parameter	Submarine Landslide			Remarks
	Area A	Area B	Area C	
$\gamma(-)$	1.4	1.4	1.4	According to the literature
b (m)	21,200	9,600	7,000	Length of sliding mass (map-reading)
T (m)	60	130	150	Depth at the peak of collapsed part (map-reading)
w (m)	3,800	6,200	6,000	Width of collapsed part (map-reading)
d (m)	590	700	400	Initial depth of sliding mass (map-reading)
θ (deg.)	1.1	1.7	1.4	Inclination of sliding mass (map-reading)
g (m/s ²)	9.8	9.8	9.8	
Cm	1	1	1	
S (m)	17,700	15,200	5,900	Distance between peak of collapsed part and peak of sedimentary part (map-reading)
S ₀ (m)	8,850	7,600	2,950	=S/2
Cn	0.009	0.086	0.072	=S ₀ / (Rcos θ)
R (m)	936,333	88,615	40,833	=b ² / 8T
a ₀ (m/s ²)	0.015	0.140	0.118	=S ₀ / t ₀ ²
t ₀ (sec)	757	233	158	From Eq. (7)
λ_0 (m)	57,573	19,292	9,899	From Eq. (8)
$\Delta\Phi$ (rad)	0.019	0.172	0.144	2S ₀ / R
u _{max} (m/s)	11.69	32.63	18.66	=S ₀ / t ₀
ΔX (m)	28,786	9,646	4,950	= λ_0 / 2
κ'	0.687	0.625	0.898	
$\eta_{0,2D}$ (m)	1.12	9.79	9.65	From Eq. (9)
$\eta_{0,3D}$ (m)	0.07	2.38	3.64	From Eq. (6)

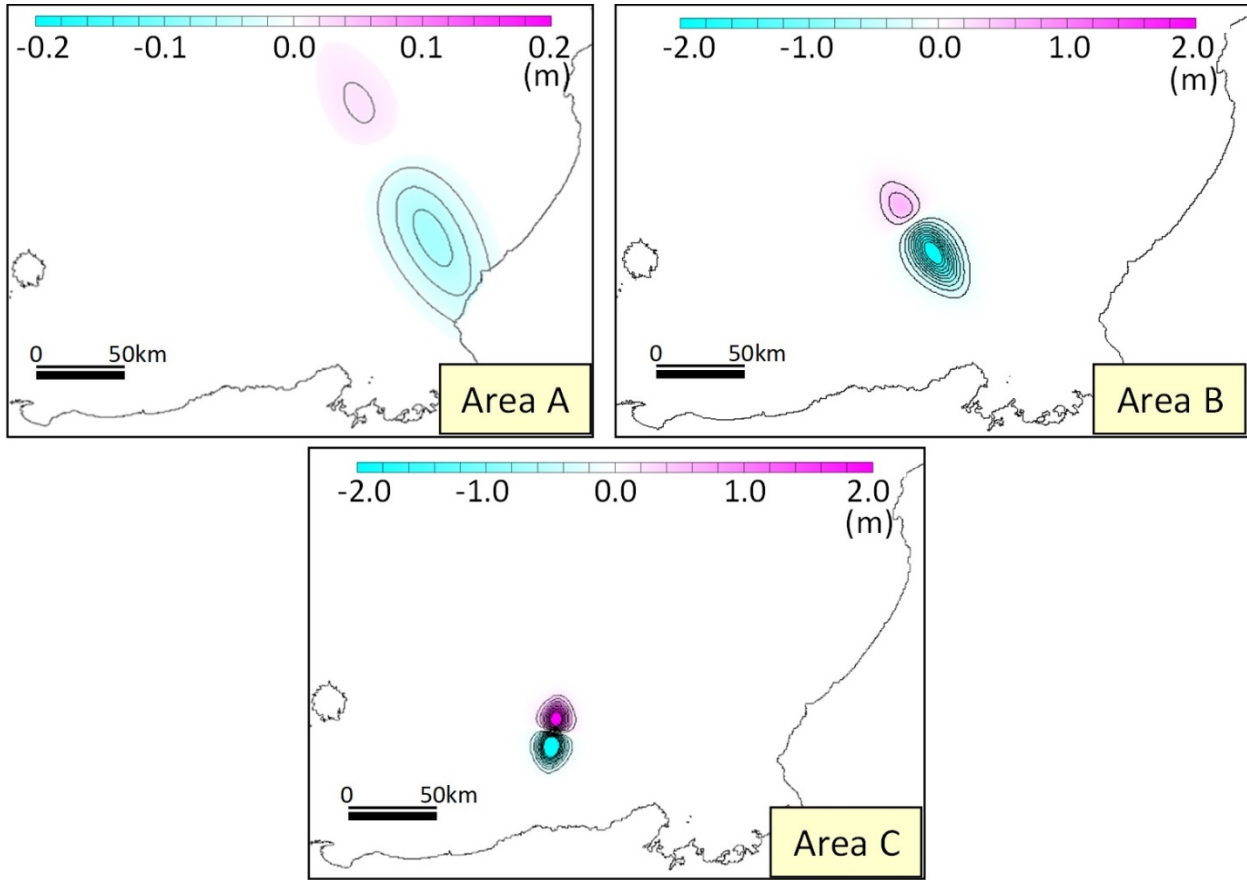


Fig. 8. Initial spatial water level distribution of submarine landslide estimated by Watts model

Table 3. Calculation conditions applied to the KLS model

Parameters	Settings		
	Area A	Area B	Area C
Grid spacing	450m		
Vertical rupture propagation velocity	0.3m/s	1.0m/s	0.5m/s
Collapse duration time	3min.	2min.	5min.

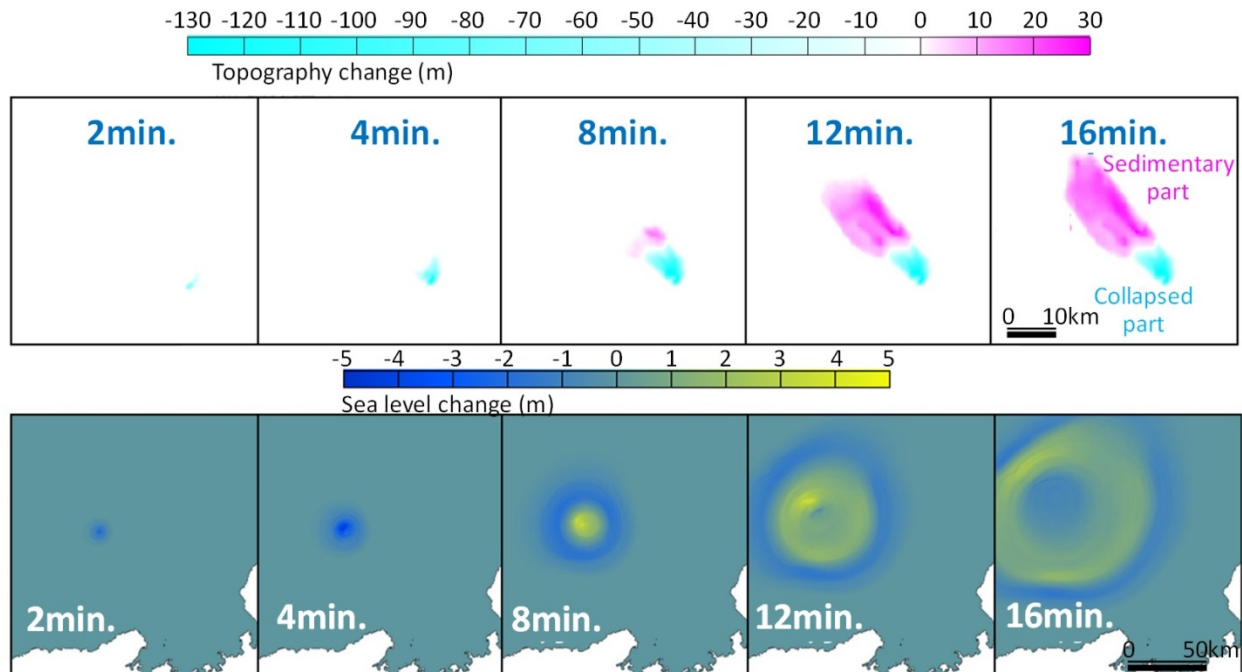


Fig. 9. Time series variation of topographical change (above) and tsunami propagation (below) calculated by KLS model in Area B

According to this, until about 4 minutes after the beginning of the landslide, only the collapse advances, without any sedimentation, and correspondingly the water level is unilaterally depressed. The water level then begins to rise, after 8 minutes, synchronously with the beginning of sedimentation.

Figure 10 shows the time series variation of topographical change and tsunami propagation calculated by the modified-KLS model in Area B. Compared to the results of the KLS model shown in Fig. 9, the water level fluctuation at each corresponding time is generally small. Also, 4 minutes from the beginning of the landslide, uplift of the water level appears in the northeastern part of the tsunami, which expanded concentrically. This is due to the fact that collapse and sedimentation are proceeding simultaneously by doubling the rupture starting point in the modified-KLS model, and it is considered also that the water surface depression due to collapse and the uplift due to sedimentation cancel each other.

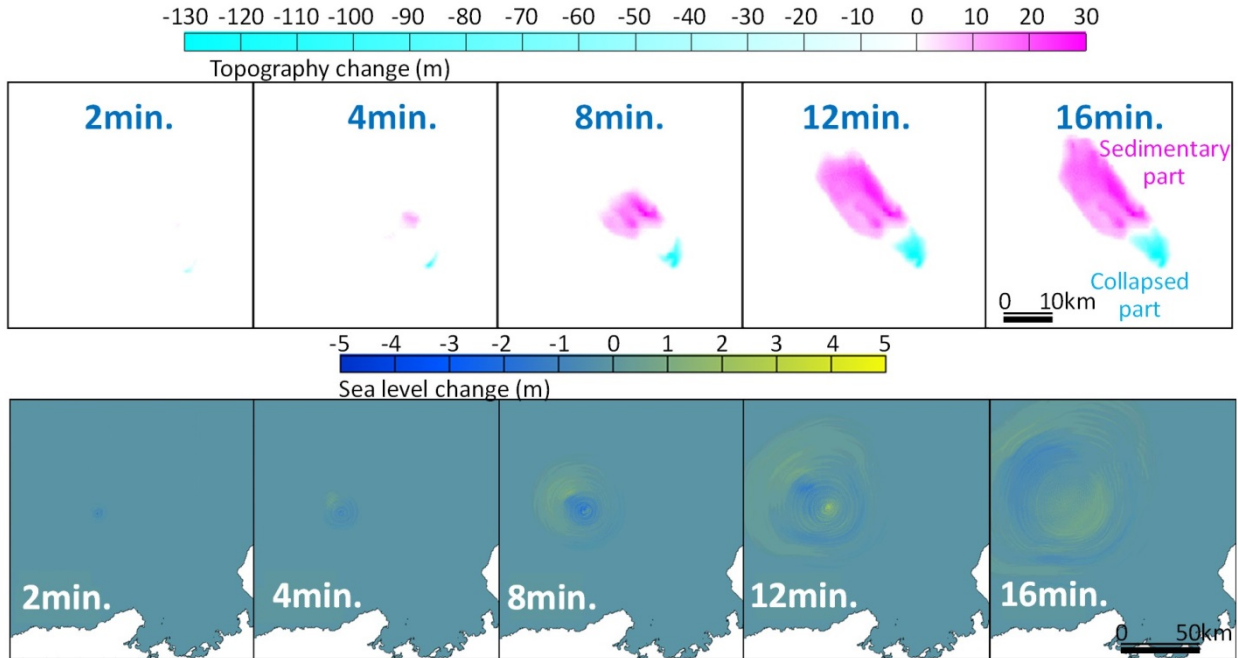


Fig. 10. Time series variation of topographical change (above) and tsunami propagation (below) calculated by modified-KLS model in Area B

For every calculation scheme, the general method of non-linear long wave theory (shallow water theory) computed by differentiating the staggered Leap-frog scheme was applied to calculate tsunami propagation.

Where the minimum space grid size : 3.125 m, time step for calculation : 0.05 s, computation time : 3 h, Manning's roughness coefficient : 0.03, tide level for tsunami height evaluation : T.P.+0.49 m (considering mean HWL for upside calculation) and T.P.-0.01 m (considering mean LWL for downside calculation) are applied as the calculation conditions, respectively.

5. DISCUSSION

The results of the tsunami height evaluation on the front of the intake of the Takahama NPP are summarized in Table 4. This shows that the evaluation result by the KLS model has a high impact on the evaluation point in every case, and the tsunami height calculated by the modified-KLS model has almost equivalent results as those of the Watts model at both the highest and the lowest water level, and only the result calculated by the KLS model obviously became large in Areas B and C. Also, in Area A, the result calculated by the KLS model was the maximum as in other areas, even though the result of the Watts model is small and the results of the KLS model and the modified-KLS model are relatively close.

Table 4. Results of the tsunami height evaluation

Tsunami Source		Evaluation Model	Tsunami Height	
			Highest (T.P. m)	Lowest (T.P. m)
Submarine Landslide	Area A	Watts	0.6	-0.1
		KLS	1.7	-0.9
		modified-KLS	1.5	-0.9
	Area B	Watts	1.9	-1.0
		KLS	3.4	-3.0
		modified-KLS	1.9	-1.0
	Area C	Watts	1.6	-1.0
		KLS	2.8	-1.7
		modified-KLS	1.2	-0.8

Based on the above results, it is not easy to reasonably set the landslide velocity and the rupture duration time in practice, since there are no detailed observation records of the submarine landslide, as pointed out by Tonomo et al. (2015). Therefore, it is difficult to reasonably evaluate possible future submarine landslides in the scheme of reproductive calculation of the submarine landslide-triggered tsunami proposed by the previous studies. On the other hand, applying the sliding velocity and the rupture duration time estimated by the method of Watts et al. (2005), it was suggested that from the viewpoint of tsunami height evaluation triggered by a future submarine landslide, approximately reasonable results are obtained by the Watts model and/or the modified-KLS model. However, for the Watts model, depending on the features of the submarine landslide topography, the possibility of obtaining a tsunami height considerably smaller than that of the other two models cannot be denied. On the other hand, since the KLS model always provides a relatively large tsunami height, it might be suitable for obtaining the tsunami height on a sufficiently safe-side in particular. The modified-KLS model seems to be a well-balanced model that can obtain a moderate tsunami height in comparison with that of the other two models. The evaluation scheme for submarine landslide-triggered tsunami height proposed in this study is applicable in practice.

6. CONCLUSION

In this study, we estimated the scale of submarine landslides from a literature survey and showed examples of tsunami height evaluation using multiple schemes. The main conclusions are as follows:

- i) A procedure was proposed to set submarine landslide properties, taking into account uncertainties of location and scale. For the evaluation target of a tsunami triggered by a submarine landslide in the waters around Wakasa Bay, the largest landslide topography was selected in each of three areas.
- ii) Three schemes were applied to calculate the initial tsunami distribution, and the setting procedure for the necessary parameter was proposed for each scheme. As a result of the tsunami height evaluation by the three schemes of the Watts model, the KLS model and the modified-KLS model, the result obtained by the KLS model was comparatively large for every case.
- iii) As a result of applying the modified-KLS model to the study case in Area B where the largest tsunami height was estimated by the KLS model at Takahama Nuclear Power Plant, the result obtained was almost equivalent to the result from the Watts model, and only the result of the KLS model was obviously larger.

- iv) From the above, the KLS model, applying the maximum sliding velocity calculated by the Watts model as a parameter, was considered to provide a larger result than those of the other two models or experimental results. Therefore, it is considered that evaluation results on the safe side can be obtained by adopting the KLS model for evaluating tsunami height triggered by a submarine landslide.
- v) Finally, the validity of the time-series variation of landslide-triggered tsunami calculated by each model should be verified in another study.

REFERENCES

- Agency for Natural Resources and Energy, 2014. 4th Strategic Energy Plan (provisional translation), METI, Government of Japan, April 2014, p.9.
- Grilli, S.T., and P. Watts, 2005. Tsunami Generation by Submarine Mass Failure. I : Modeling, Experimental Validation, and Sensitivity Analysis, *Journal of Waterway, Port, Coastal, and Ocean Engineering*, ASCE, pp.283-297.
- Hashimoto, T. and K. Dan, 2008. Experimental study on submarine landslide tsunami in various landslide mass shapes, *Abstract of JSCE Annual Meeting*, Vol. 63, No. 2, pp.395-396. (in Japanese)
- Hiraishi, T, H. Shibaki and N. Hara, 2001. Reproduction calculation of Meiwa-Yaeyama earthquake tsunami by applying circular slip method as submarine landslide tsunami source, *Annual Journal of Coastal Engineering*, JSCE, Vol. 48, pp.351-355. (in Japanese)
- Ikehara, K., H. Katayama and M. Sato, 1990. Sedimentological Map Offshore of Tottori, *Marine Geological Map*, No. 36, Geological Survey of Japan. (in Japanese)
- Katayama, H., M. Sato and K. Ikehara, 1993. Sedimentological Map Offshore of Kyō-ga-Misaki, *Geological Map*, No. 38, Geological Survey of Japan. (in Japanese)
- Katayama, H., M. Sato and K. Ikehara, 2000. Sedimentological Map Offshore of Gentatsu-se, *Geological Map*, No. 53, Geological Survey of Japan. (in Japanese)
- Matsuyama, M, K. Satake and T. Matsumoto, 2001. Reflection seismic survey in the source region of Papua New Guinea tsunami in 1998 and parameter study by numerical calculation, *Annual Journal of Coastal Engineering*, JSCE, Vol. 48, pp.366-370. (in Japanese)
- Satake, K. and Y. Kato, 2002. The 1741 Japan Sea tsunami caused by debris avalanche in the Toshima-Oshima volcano, *Kaiyo monthly/special*, No. 28, pp.150-160. (in Japanese)
- Tokuyama, E., E. Honza, M. Kimura, S. Kuramoto, J. Ashi, Y. Okamura, H. Arato, Y. Itoh, W. Soh, R. Hino, T. Nohara, H. Abe, S. Sakai and K. Mukaiyama, 2001. Tectonic development in the regions around Japan since latest Miocene, *Journal of Japanese Society for Marine Survey and Technology*. (in Japanese)
- Tonomo, K., T. Shikata and Y. Murakami, 2015. Accuracy study of numerical simulation of tsunami applied to the submarine landslide model, *Journal of JSCE, Ser. B3 (Ocean Engineering)*, Vol.71, No.2, pp.I_557-I_562. (in Japanese)
- Watts, P., S.T. Grilli, D.R. Tappin, and G.J. Fryer, 2005. Tsunami Generation by Submarine Mass Failure. II: Predictive Equations and Case Studies, *Journal of Waterway, Port, Coastal, and Ocean Engineering*, ASCE, pp.298-310.
- Yamamoto, H., M. Joshima and K. Kishimoto, 1989. *Geological Map Offshore of Tottori*, Marine Geological Map, No. 35, Geological Survey of Japan. (in Japanese)
- Yamamoto, H., M. Joshima and K. Kishimoto, 1993. *Geological Map Offshore of Kyo-ga Misaki*, Marine Geological Map, No. 40, Geological Survey of Japan. (in Japanese)
- Yamamoto, H., M. Joshima and K. Kishimoto, 2000. *Geological Map Offshore of Gentatsu-se*, Marine Geological Map, No. 50, Geological Survey of Japan. (in Japanese)
- Yamamoto, H., 1991. A submarine sediment slide on the continental slope off Fukui Prefecture, Southern Japan Sea, *Bulletin of the Geological Survey of Japan*, Vol. 42, No. 5, pp.221-232. (in Japanese)